Joule heating and current-induced domain wall motion

J. Curiale, A. Lemaître, T. Niazi, G. Faini, and V. Jeudy

Citation: J. Appl. Phys. **112**, 103922 (2012); doi: 10.1063/1.4765032
View online: http://dx.doi.org/10.1063/1.4765032
View Table of Contents: http://jap.aip.org/resource/1/JAPIAU/v112/i10
Published by the American Institute of Physics.

Joule heating and current-induced domain wall motion

J. Curiale,[1,2,3] A. Lemaître,[2] T. Niazi,[2] G. Faini,[2] and V. Jeudy[1,4,a)]
[1]*Laboratoire de Physique des Solides, Université Paris-Sud, CNRS, 91405 Orsay, France*
[2]*Laboratoire de Photonique et de Nanostructures, CNRS, 91460 Marcoussis, France*
[3]*Centro Atómico Bariloche, Comisión Nacional de Energía Atómica, Avenida Bustillo 9500 & Consejo Nacional de Investigaciones Científicas y Técnicas—CONICET, CCT-Comahue, Quintral 1250, 8400 S. C. de Bariloche, RN, Argentina*
[4]*Université Cergy-Pontoise, 95000 Cergy-Pontoise, France*

(Received 11 April 2012; accepted 12 October 2012; published online 28 November 2012)

We investigate numerically and experimentally the Joule heating produced by current pulses and its contribution to current-induced domain wall (DW) motion in a (Ga,Mn)As ferromagnetic semiconductor. Different thermal coupling between tracks and substrates are explored. A direct contact leads to a logarithmic transient temperature rise and a stationary state determined by the substrate thickness. The introduction of a low thermal conducting (Ga,In)As interlayer produces an additional temperature rise whose time variation and magnitude are analyzed. Experimentally, the measured temperature rises present a good agreement with predictions over more than four orders of magnitude in time for values of the heat conductivity and of the heat capacity close to those reported in the literature. The Joule heating is shown to produce non-linearities in the domain wall velocity versus current density characteristics. A correction of Joule heating is proposed and permits the identification of the flow regimes from a comparison of domain-wall dynamics in tracks presenting different pinning characteristics. © *2012 American Institute of Physics*. [http://dx.doi.org/10.1063/1.4765032]

I. INTRODUCTION

Magnetization reversal can be produced by an electrical current in ferromagnetic systems such as spin valves or magnetic tracks. Indeed, the spin of the itinerant current-carrying charges exert torques on the localized magnetic moments.[1] These so-called spin-transfer torques (STT) could be at the basis of magnetic memory and logic devices,[2,3] giving rise to many applied and fundamental physics researches.[4] However, current produces Joule heating, associated with temperature rises and gradients. These temperature variations affect, in turn, the static and dynamical properties of ferromagnetic materials and contribute to the magnetization reversal.

In magnetic tracks, magnetization reversal results from the current-induced domain wall (DW) motion. The current densities required to observe STT effects are rather large. Typical threshold values are of the order of 10^9 A/m^2 and 10^{12} A/m^2, for semiconducting[5–9] and metallic[10] tracks, respectively. Temperature rises of a few Kelvins or a few tens of Kelvin have been reported in the literature.[6,11–13] Hence, Joule heating appears as a limiting factor to the investigation of spin transfer torque phenomena. Temperature rises can be sufficiently large to cross the Curie temperature or even to deteriorate the tracks. Also, in Ref. 14, the Joule heating contribution to current-induced DW-motion was shown to be larger than the STT contribution. Therefore, heating has to be taken into account to analyze properly the current-induced domain wall dynamics in thermally activated and flow regimes.[5,8] To the best of our knowledge, the interplay between current-induced DW-motion and Joule heating remains to be explored.

Joule heating produced by current pulses in tracks was studied theoretically.[15–18] The transient heating regime was examined in Ref. 15 for a track sitting on a semi-infinite substrate. An analytical expression of the stationary temperature rise is proposed in Ref. 16 for a finite substrate thickness. More recently, Curiale *et al.*[18] have studied numerically and experimentally the temperature rises produced by Joule heating in (Ga,Mn)(As,P) tracks grown on a GaAs substrate. The temperature rise in the transient regime was shown to exhibit a logarithmic variation with the current pulse duration. The maximum temperature rise corresponding to the steady state regime was shown to be controlled by substrate thickness.

A thin insulating interlayer is often inserted between the track and the substrate. For example, this ensures electrical insulation and confines charge carriers in the ferromagnetic track. For (Ga,Mn)As, the magnetic layer has to be under tensile strain to get a perpendicular magnetized layer. This configuration is achieved by using a relaxed (Ga,In)As interlayer.[19] Interlayers with lower heat conductivity than the substrate enhance the track temperature rise. The contribution of a lower thermal conducting interlayer was considered theoretically in Ref. 17 for a semi-infinite substrate. This question has been hardly explored experimentally.

In this paper, we propose an extensive study of Joule heating for different thermal coupling between a track and a substrate. We also explore the contribution of temperature rises to DW dynamics in the flow regime. The paper is organized as follows. Part II describes the geometries, the thermal parameters and the finite element method (FEM) used to study Joule heating. The predictions of the simulations for different interlayer thicknesses and different track widths are presented and compared to analytical predictions[15–17] in Part III. Part IV details the experimental studies

a)Electronic mail: vincent.jeudy@u-psud.fr.

of Joule heating in the stationary and the transient heating regimes. The contribution of Joule heating on current-induced DW-motion is analyzed in part V.

II. METHODS

A. Samples

In order to study the thermal coupling between the tracks and their substrate, different samples were elaborated containing or not an interlayer. The magnetic layer thickness is identical for all the samples $h = 50$ nm. The samples without interlayer (samples 1a and 1b) consist of annealed $(Ga_{0.90}Mn_{0.10})(As_{1-y}P_y)$ films,[20] grown by molecular beam epitaxy on a GaAs (001) substrate (thickness $L = 375\ \mu$m). For sample 1a, $y = 0.11$ and for sample 1b, $y = 0.07$. The microtracks were patterned by e-beam lithography with length $l = 90\ \mu$m, and different widths $w = 0.5$, 1, 2, 4 μm.[9] A top view of the tracks is shown in Fig. 1(a). The Curie temperatures $T_c^{1a} = 110.0$ K and $T_c^{1b} = 120.0$ K were deduced from the vanishing polar magneto-optical Kerr (PMOKE) contrast and from the maximum of the differential resistivity curves. The resisitivity $\rho^{1a} = 62.8\ \mu\Omega$ m and $\rho^{1b} = 51.3\ \mu\Omega$ m, at 100–110 K. Sample 2 is an annealed $Ga_{0.93}Mn_{0.07}As$ film grown on a (Ga,In)As interlayer (thickness $d = 2.5\ \mu$m), itself deposited on a GaAs (001) substrate ($L = 375\ \mu$m).[19] The In concentration gradually increases in the first 0.5 μm from 0% to 10% and then remains constant at 10% over the upper 2 μm. Tracks, 90 μm long and 4 μm wide, were also patterned by e-beam lithography ($T_c = 114$ K). The resistivity $\rho = 44.5\ \mu\Omega$ m close to 100 K. The experiments on Joule heating were performed in an open cycle optical cryostat with a temperature accuracy of 0.2 K. The substrates were fixed with silver paint to different alumina sample holders. The whole set was fixed also with silver paint to the cold plate of the cryostat. Studies on current-induced domain wall dynamics performed with samples 1 and 2 are reported in Refs. 6, 8, and 9.

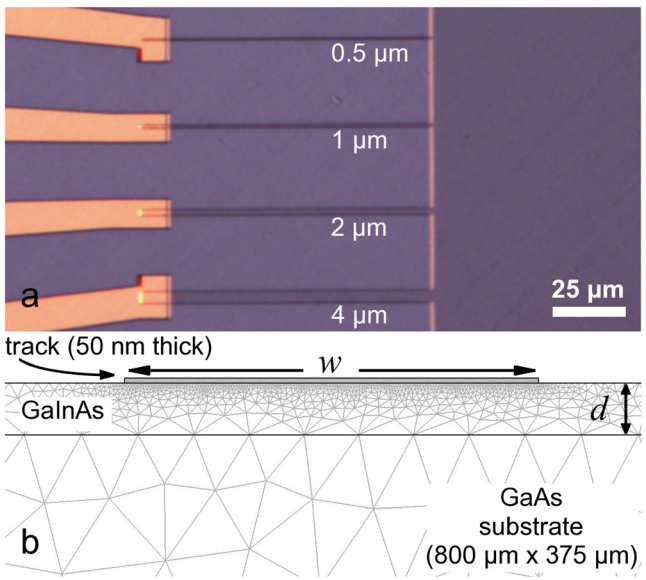

FIG. 1. (a) Top view of the four (Ga,Mn)(As,P) tracks with different widths ($w = 0.5$, 1, 2, 4 μm) showing the gold contacts (left) and a (Ga,Mn)(As,P) pad (right). (b) Cross-section view featuring the track (width w), the (Ga,In)As interlayer (thickness d), the GaAs substrate, and the mesh used to solve the diffusion equation numerically.

B. Numeric simulations

The geometry used for the simulations is presented in Fig. 1(b). The studied structure consists in an infinitely long track of thickness $h = 50$ nm sitting on an interlayer ((Ga,In)As) of thickness d. The substrate (GaAs), underneath the interlayer, is $L = 375\ \mu$m thick. Different track widths ($w = 1$, 2, and 4 μm) and interlayer thicknesses (d = 0, 0.5, 1.25, and 2.5 μm) were simulated.

The Joule heating produced by an electrical current is deduced from the heat diffusion equation

$$\rho_s C \frac{\partial T(\mathbf{r},t)}{\partial t} - K\nabla^2 T(\mathbf{r},t) = S(\mathbf{r},t), \qquad (1)$$

where ρ_s, C, K, $T(\mathbf{r},t)$ are the density, specific heat, thermal conductivity, and the temperature at the position $\mathbf{r}$ and time t, respectively. The heat source $S(\mathbf{r}, t) = P/(lwh)$ where $P(= RI^2)$ is the power dissipated by the current $I = Jwh$ in the resistance $R = \rho l/wh$. J is the current density.

The heat conductivity and heat capacity constants used in the simulations are those providing the best agreement with the experimental results. The substrate heat conductivity ($K = 140$ W/m K) is close to the value reported by Blakemore[21] for the GaAs lattice conductivity. The same value was taken into account for the track since the heat conductivity of the carrier, roughly estimated from the Wiedemann-Franz law, was found more than three orders of magnitude lower than the lattice conductivity. For the interlayer, the heat conductivity is $K_i = 10$ W/m K. This value, much lower than K, is compatible with alloying effects in (Ga,In)As, as reported in Ref. 22. The heat capacity $C = 200$ J/kg K ($\rho_s = 5.33$ g/cm^3)[21] was assumed to be identical for the track, the interlayer, and the substrate. This assumption is not critical since the variation of the specific heat with the doping is no significant for the considered doping concentrations and temperatures.[23]

The simulations were performed in two dimensions as $l \gg w$. Indeed, simple solid angle considerations indicate that the heat escaping through the track ends ($\propto D8wh/(l^2)$, where $D = K/(\rho_s C)$ is the heat diffusion coefficient) is close to 5 orders of magnitude smaller than the heat diffusion through the substrate ($\propto 2\pi D$), except close to the edges where temperature rises are weaker. The heat diffusion equation was solved with a FEM commercial software.[24] In order to reduce the calculation time, the mesh size was optimized (see Fig. 1(b)) and the GaAs substrate width was limited to 800 μm. We checked that reducing the mesh size and/or changing the substrate width had no significant effect on the track temperature.

III. THEORETICAL INVESTIGATIONS

A. Track heating without interlayer

The current is applied at $t = 0$, the track temperature increases with time $T(t) = T_i + \Delta T(t)$, due to Joule heating. T_i is the initial track temperature. The temperature rise

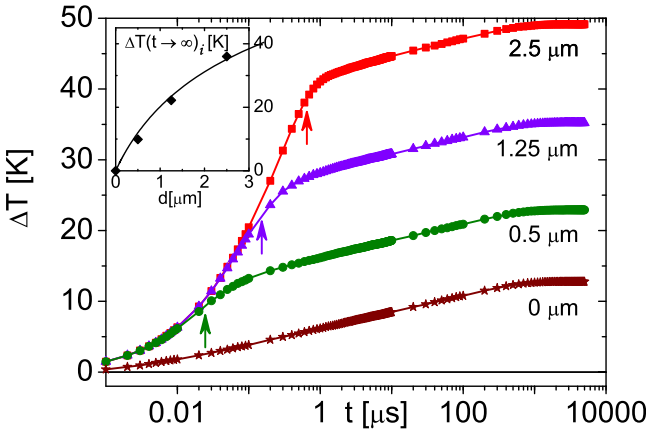

FIG. 2. Predicted temperature rises ΔT versus time at the center of a 4 μm wide track and for different interlayer thicknesses ($d = 0$, 0.5, 1.25, 2.5 μm). The arrows indicate the diffusion time in the interlayer t_{Di} for the different d-values. Inset: Comparison between the predictions of Eq. (4) and the simulation for the maximum interlayer temperature rise $\Delta T(t \to \infty, d)_i = \Delta T(t \to \infty, d) - \Delta T(t \to \infty, d = 0\,\mu\text{m})$. Resistivity: $\rho = 44.5\,\mu\Omega$m, current density: $J = 10\,\text{GA/m}^2$.

$\Delta T(t)$, taken at the track center, is shown in Fig. 2 for different interlayer thicknesses. Without interlayer ($d = 0\,\mu$m), $\Delta T(t)$ varies logarithmically with t, in the transient regime. This is in agreement with the theoretical predictions of You *et al.*[15,17]

$$\Delta T(t) = \frac{P}{2\pi K l}\left[\ln\left(\frac{16D}{w_G^2}\right) + \ln t\right] \tag{2}$$

valid for $t \gg w_G^2/D$, where w_G is the width of the assumed Gaussian heat profile ($w_G \approx w$).[15] The logarithmic variation originates from the quasi radial heat propagation from the track to the substrate, during the transient regime. The stationary regime is reached for $t \approx 1$ ms. The corresponding diffusion length $l_D = \sqrt{Dt} = 360\,\mu$m is close to the thickness of the substrate ($L = 375\,\mu$m): the time $t_D = L^2/D$ required to reach the stationary regime is determined by the heat diffusion through the full substrate thickness.

For the stationary regime, the average temperature rise of the track ($\Delta T(t \to \infty)$) was calculated by Kim *et al.*[16] The prediction for a sufficiently thick substrate ($L \gg w$) is

$$\Delta T(t \to \infty, d = 0\ \ \mu\text{m}) = \frac{P}{\pi K l}\left[\frac{3}{2} + \ln\left(\frac{2L}{w}\right)\right]. \tag{3}$$

For $J = 10\,\text{GA/m}^2$, the maximum track temperature increase calculated from Eq. (3) is $\Delta T(t \to \infty, d = 0\,\mu\text{m}) = 13.5$ K. This is close to the value ($\Delta T(t \to \infty,\ d = 0\,\mu\text{m}) = 13$ K) deduced from numerical simulations. Therefore, Eqs. (2) and (3) provide rather accurate predictions for the transient and stationary heating regimes of the track.

B. Contribution of the interlayer to Joule heating

When an interlayer with a lower heat conductivity is inserted between the track and the substrate ($d \neq 0\,\mu$m), larger temperature rises are obtained. As shown in Fig. 2, different heating regimes can be distinguished. For $t < 20$ ns, the three curves obtained for $d \neq 0\,\mu$m are superimposed and the slope $\Delta T(t)/ln(t)$ is higher than for $d = 0\,\mu$m. This reflects the heating of the interlayer. As indicated by arrows in Fig. 2, the time elapsed until the curves leave this initial common variation increases with d. This time almost coincides with the diffusion time in the interlayer $t_{Di} = d^2/D_i$ ($t_{Di} = 25$, 150 650 ns for $d = 0.5$, 1.25 and 2.5 μm, respectively). Therefore, for $t < t_{Di}$, the temperature rises are dominated by the heating of the interlayer.

For $t > t_{Di}$, the slopes $\Delta T(t)/ln(t)$ obtained for $d \neq 0\,\mu$m are close to the slope found for $d = 0\,\mu$m. This indicates that the temperature rises are dominated by the heat diffusion through the substrate. The temperature rise reached in the stationary regime increases with the interlayer thickness d, as shown in Fig. 2. The contribution of the interlayer to the maximum temperature rise ($\Delta T(t \to \infty, d)_i = \Delta T(t \to \infty, d) - \Delta T(t \to \infty,\ d = 0\,\mu m)$) is reported in the inset of Fig. 2 as a function of d. The average temperature rise of track in the stationary regime was calculated by Kim *et al.*[16] for an interlayer of thickness d in contact with a thermostat:

$$\Delta T(t \to \infty, d)_i = \frac{P}{\pi K_i l}\,\xi\left(\frac{w}{2d}\right), \tag{4}$$

where $\xi(\alpha) = (1/4)\left(ln(1 + \alpha^{-2}) - \alpha^{-2} ln(1 + \alpha^2)\right) + \alpha^{-1} tan^{-1}\alpha$. The comparison of this analytical prediction with the results of the simulations is reported in the inset of Fig. 2. The good agreement reflects the large difference between the heat conductivities of the substrate and the interlayer.

Here, it is important to emphasize that the main features of the temperature rises reported in Fig. 2 can be almost reconstructed using the set of Eqs. (2)–(4) and the diffusion times. The slopes can be deduced from Eq. (2). The steady state temperature increases is given by Eqs. (3) and (4). The end of the transient heating regimes corresponds to the diffusion times through the interlayer and the substrate. Note that a bad thermal link between the substrate leads to larger track temperature rises and delays the achievement of the stationary regime.

Steady state temperature profiles along the direction perpendicular to the track are reported in Fig. 3 for different interlayer thicknesses. They correspond to temperatures calculated at the top of the interlayer. The temperature rises ΔT extends over distances much larger than the track width ($w = 4\,\mu$m). Far from the track ($>10\,\mu$m), the curves obtained for different d-values are superimposed with the curve obtained without interlayer ($d = 0\,\mu$m): the temperature profile is mainly determined by the heat diffusion through the substrate. Close to the track, ΔT increases strongly with d: $\Delta T = 13$ K for $d = 0\,\mu$m while $\Delta T = 49$ K for $d = 2.5\,\mu$m. This results from the low heat conductivity of the interlayer, which confines heat below the track.

Within the track, the temperature profiles present larger gradients when increasing the interlayer thickness, as shown in Fig. 3. Without any interlayer, the track heating is rather homogeneous, within a few hundredths of Kelvins, while the temperature gradients can reach several Kelvins per micron for thick interlayers ($d \geq 1\,\mu$m). Thermally activated processes as domain wall creep, domain nucleation will be

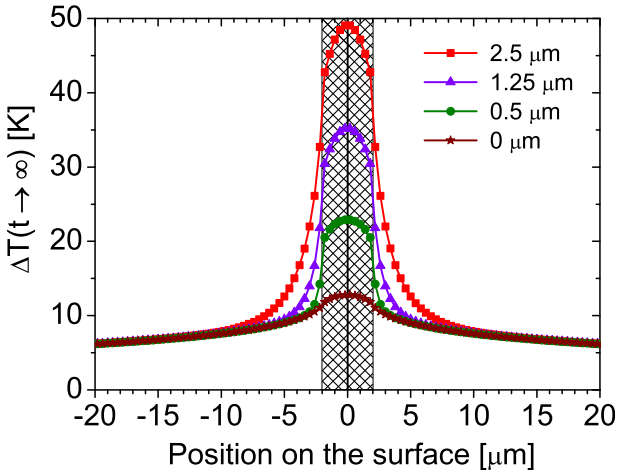

FIG. 3. Temperature profiles in the steady regime for different interlayer thicknesses ($d = 0$, 0.5, 1.25, 2.5 μm). The profiles are taken on the top of the interlayer, in the direction perpendicular to the track. Increasing d increases the heat confinement and the temperature T of the track. The shaded area between $-2\,\mu$m and $+2\,\mu$m features the width of the track. Resistivity: $\rho = 44.5\,\mu\Omega$m, current density: $J = 10\,\mathrm{GA/m^2}$, initial temperature: $T = 100\,\mathrm{K}$.

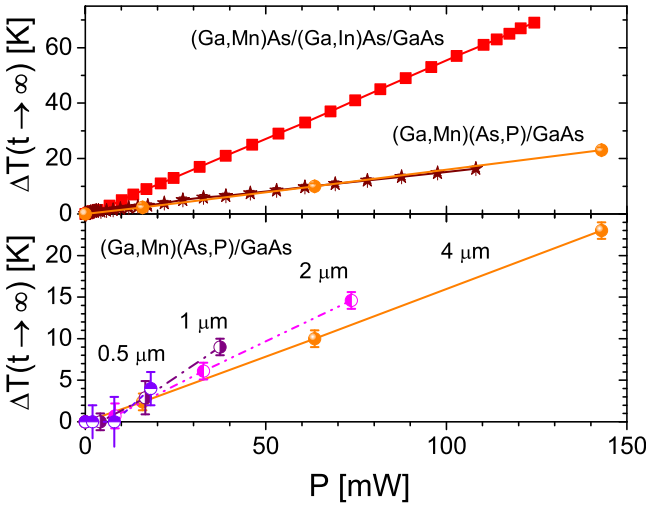

FIG. 4. Measured temperature rises $\Delta T(t \to \infty)$ in the stationary regime as a function of the power dissipated by Joule effect, for different sample architectures. (Top) Comparison between different 4 μm wide tracks. Squares (sample 2): (Ga,Mn)As track deposited on a ($d =$) 2.5 μm thick (Ga,In)As interlayer. Circles (sample 1a) and stars (sample 1b): (Ga,Mn)(As,P) tracks with two different P concentration directly deposited on a GaAs substrate ($d = 0\,\mu$m). (Bottom) Comparison between (Ga,Mn)(As,P) tracks of different widths ($w = 0.5$, 1, 2, 4 μm) directly deposited on a GaAs substrate (sample 2).

enhanced in the track center part. In the uttermost case, this part would enter the paramagnetic phase while the track edges would remain ferromagnetic. Similarly, along the track length, three dimensional simulations indicate that the temperature rise is larger close to the center than to its ends. The deviation from homogeneous temperature is of the order of $\pm 6\%$ for 85% of the track length around the central part. This should favor domain wall motion towards the center of tracks, as reported in Ref. 25.

To conclude this part, we shall comment on experiments performed in metallic tracks deposited on SiO_2 interlayers.[14,15,26–28] Typically, the native oxide thickness at the surface of a Si substrate is of the order of 2 nm. A SiO_2 layer ($d \approx 100\,\mathrm{nm}$) can also be intentionally grown up in order to provide electrical insulation. However, the low heat conductivity of SiO_2 ($K_i \approx 1\,\mathrm{W/m\,K}$) should enhance the temperature rises. An estimation can be deduced from Eqs. (3) and (4), for the typical current threshold required to produce DW-motion ($J \approx 10^{12}\mathrm{A/m^2}$) and using the sample characteristics reported in Ref. 17 ($\rho = 7.25\,\mu\Omega\,\mathrm{cm}$, $w = 200\,\mathrm{nm}$, $h = 10\,\mathrm{nm}$, and $K = 130\,\mathrm{W/mK}$). Without interlayer, the temperature rise of the track $\Delta T(t \to \infty, d = 0\,\mathrm{nm}) \approx 3\,\mathrm{K}$. A SiO_2 interlayer adds a contribution $\Delta T(t \to \infty,\ d = 100\,\mathrm{nm})_i \approx 26\,\mathrm{K}$. Hence, a 100 nm thick SiO_2 interlayer provides the major contribution to the temperature rise of tracks. This contribution should be even more pronounced in the transient regime.

IV. EXPERIMENTAL INVESTIGATIONS

A. Stationary regime

In the stationary regime, the temperature rise $\Delta T(t \to \infty)$ was measured by monitoring the track temperature dependent resistivity.[18] $\Delta T(t \to \infty)$ was measured at constant track temperature ($T = 100\,\mathrm{K}$, i.e., at constant resistivity): for each current density J, the initial sample temperature was set to $T_i = T - \Delta T(t \to \infty, J)$ in order to compensate for Joule heating. Experimental results are reported in Fig. 4.

For all the samples, $\Delta T(t \to \infty)$ is found to be proportional to the power P dissipated by the current in the track as predicted for pure Joule heating effect. The superimposition of results obtained for both samples (samples 1 a and 1 b) with the same architecture and different resistivity corroborates this conclusion. The best fit with the simulations was obtained for $K = 140\,\mathrm{W/m\ K}$. The hole contribution to the heat diffusion, estimated from the Wiedemann-Franz law, is 3–4 orders of magnitude lower than the lattice contribution. The obtained heat conductivity is, therefore, associated to GaAs lattice conductivity. This value is also compatible with GaAs lattice conductivity reported in Ref. 21 ($K = 170$–$240\,\mathrm{W/m\ K}$, for $T = 100\,\mathrm{K}$). Hence, the steady state track temperature rise is controlled by the heat diffusion through the substrate.

Temperature rises measured for different track widths w are also reported in Fig. 4 (bottom). The slope $\Delta T(t \to \infty)/P$ increases with decreasing w, as predicted by Eq. (3): the thermal coupling between the track and the substrate is reduced for smaller track widths.

For the sample with the interlayer (sample 2), the temperature rise is larger, a consequence of the interlayer lower heat conductivity. The best fit is obtained for an interlayer heat conductivity $K_i = 10\,\mathrm{W/m\,K}$. Such a strong reduction of the heat conductivity is most probably due to the (Ga,In) alloying effect. Indeed, for In concentration $y \sim 10$ %, Ref. 22 gives a heat conductivity ratio $K/K_i \approx 3$ for $T = 300\,\mathrm{K}$. The ratio, obtained for $T = 100\,\mathrm{K}$, is much larger ($K/K_i = 14$), and could be associated to the weaker temperature variation of the heat conductivity in alloys due to disorder scattering.

B. Transient regime

The transient temperature rise $\Delta T(t)$ was deduced from the probability of the Joule heat pulse to induce magnetization reversal in an homogeneously magnetized track as its temperature crosses the nucleation temperature T_{nuc}. T_{nuc} is slightly smaller than the Curie temperature T_c since the homogeneous magnetized state is a metastable state. Before the pulse, the track temperature was set to $T = T_{\mathrm{i}}$ below T_c. The track was prepared in a homogeneous magnetized state, checked by magneto-optical Kerr microscopy. A small magnetic field (≈ 0.25 Oe) was used to ensure that heating above T_{nuc} results in magnetization reversal. The tracks were submitted to current pulses of constant amplitude and of increasing durations. For different initial track temperatures T_{i}, we measured the pulse duration Δt_{min} (Δt_{max}) below (above) which magnetization reversal is never (always) observed after 10 pulses ($\Delta t_{\mathrm{mean}} = (\Delta t_{\mathrm{min}} + \Delta t_{\mathrm{max}})/2$). The transient temperature rise curve could then be simply reconstructed by plotting each value of $\Delta T(t) = T_{\mathrm{nuc}} - T_{\mathrm{i}}$ vs $t = \Delta t_{\mathrm{mean}}$.

The results are shown in Fig. 5 and compared with simulations for two different values of the current density. For $1\,\mu\mathrm{s} < t < 1\,\mathrm{ms}$, $\Delta T(t)$ varies logarithmically with t, as predicted by Eq. (2) for the transient regime. The slope $(d\Delta T(t)/d\ln t)$ obtained for $J = 10\,\mathrm{GA/m^2}$ is two times larger than the slope obtained for $J = 7\,\mathrm{GA/m^2}$, reflecting the quadratic variation to $\Delta T(t)$ with J. The slopes are in good quantitative agreement with the prediction $d\Delta T(t)/d\ln t = P/2\pi Kl$, for $K = 140\,\mathrm{W/mK}$, as deduced from DC electrical measurements. The linear variations of $\Delta T(t)$ with $\ln(t)$ ends after $t \approx 1\,\mathrm{ms}$ close to the time diffusion $t_D = L^2/D = 1.1\,\mathrm{ms}$ of the heat through the substrate. At this time, the stationary regime is reached. As T_{nuc} is not known *a priori*, the curves were shifted in order to adjust maximum measured temperature rises to the values deduced for DC electrical measurements. The nucleation temperatures were found to be $T_{nuc} = T_c - 2\,\mathrm{K}$ and $T_c - 1.12\,\mathrm{K}$, for $J = 10$ and $7\,\mathrm{GA/m^2}$, respectively. The decrease of T_{nuc} with increasing J suggests that the current reduces the height of the nucleation barrier.

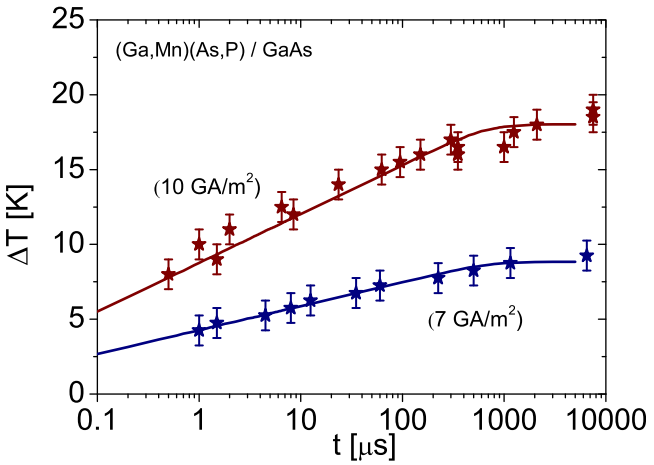

FIG. 5. Comparison between measured and predicted (lines) temperature variations ΔT versus time for a (Ga,Mn)(As,P), 4 μm wide track (sample 1b) and for two different current densities: $J = 7$ and $10\,\mathrm{GA/m^2}$. Data obtained for $J = 7\,\mathrm{GA/m^2}$ are taken from Ref. 18.

Therefore, the temperature rises measured over four orders of magnitude (1–10 000 μs) of pulses duration are in good quantitative agreement with the predictions, a strong indication that the track temperature rises are controlled by the heat diffusion through the substrate. We emphasize that the experimental investigation of heating effects over four orders of magnitude in time could not be achieved by pure electrical means.[16]

V. JOULE HEATING AND DOMAIN WALL DYNAMICS

We now investigate the contribution of Joule heating to current-induced magnetic DW dynamics. The experimental method used to determine the DW velocity has been extensively described in Refs. 5 and 6. DW displacements Δx, controlled by differential PMOKE,[6] are produced by current pulses of different amplitudes J and of constant duration Δt. Typical pulse amplitudes and durations required to produce DW-motion in the steady state propagation regime are of the order of $J \approx 10\,\mathrm{GA/m^2}$ and $\Delta t \approx 1\,\mu\mathrm{s}$, respectively.[6,8] For this time duration, tracks remains in the transient heating regime, as shown in Fig. 5. The temperature rise is significantly smaller than for the steady state. For the 4 μm wide track of sample 1 a, ((Ga,Mn)(As,P) on GaAs without interlayer) injecting $J = 10\,\mathrm{GA/m^2}$, leads to $\Delta T(1\,\mu\mathrm{s}) \approx 8\,\mathrm{K}$ while $\Delta T(t \to \infty) \approx 18\,\mathrm{K}$. On the other hand, for sample 2, ((Ga,Mn)As on a 2.5 μm (Ga,In)As interlayer), the same J-value produces $\Delta T(1\ \mu\mathrm{s}) \approx 40\,\mathrm{K}$ and $\Delta T(\infty) \approx 49\,\mathrm{K}$. The temperature rises for a 1 μs pulse duration are, therefore, rather different from those corresponding to the stationary state.

An accurate correction of the Joule heating is not straightforward. Indeed, both the thermally activated dynamical regimes and the dissipation limited regimes depend on temperature.[5,9,14] Moreover, the temperature rises vary quadratically with the current density J, i.e., each J-value is associated to a different evolution of the track temperature. An optimum correction of Joule heating would consist in a convolution of the temperature variations of the instantaneous DW velocity and the temperature increase of the track during the current pulse. However, the track temperature rise $\Delta T(J,t)$ evolves logarithmically with time. As shown in the inset of Fig. 6, for a $\Delta t = 1\,\mu\mathrm{s}$ pulse, after 0.25 μs, the temperature rise only varies by less than $\pm 13\%$. Therefore, it seems reasonable to assume the track temperature is constant during current pulses and to take as effective temperature a value close to $T = T_i + \Delta T(J, \Delta t = 1\,\mu\mathrm{s})$.

In order to determine the contribution of Joule heating to DW dynamics, current-induced domain wall motion was investigated for three different assumptions about temperature rises, as reported in Fig. 6.

Case 1 (1μs corr.): The Joule heating is corrected as discussed above. The initial track temperature $T_i(J)$ is set in such a way that the final temperature, at the end of the pulse is constant ($T_f(J) = 95\,\mathrm{K}$) whatever J. One gets $T_i(J) = 95\,\mathrm{K} - \Delta T(J, 1\,\mu\mathrm{s})$.

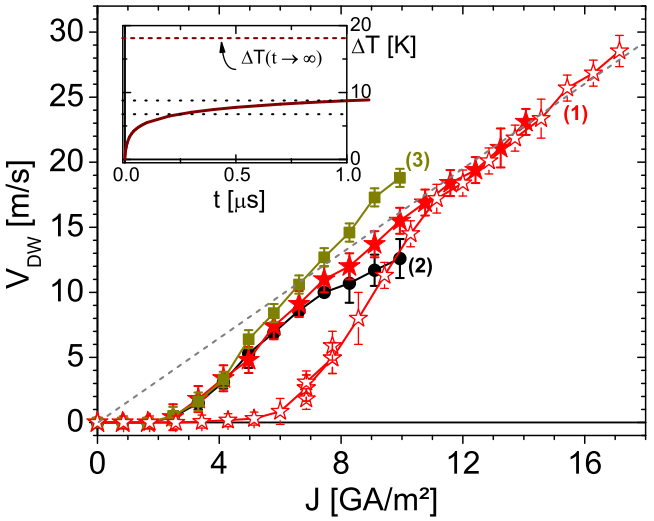

FIG. 6. Domain wall velocity as a function of the current density, measured in the 2 μm (empty symbols) and the 4 μm wide tracks (filled symbols) of sample 1a, for different final track temperatures T_f. Stars: $T_f = 95\,\mathrm{K}$ (case 1: 1 μs correction, see text). Circles: $T_f(J) = 95\,\mathrm{K} + \Delta T(J, 1\mu s) - \Delta T(J, \infty) < 95\,\mathrm{K}$ (case 2: steady state correction). Squares: $T_f = 95\,\mathrm{K} + \Delta T(J, \infty) > 95\,\mathrm{K}$ (case 3: uncorrected). Domain wall motion is always produced by 1 μs pulses. Sample 1a. Inset: Track temperature rise during a 1 μs pulse (solid line) and steady state temperature rise (dashed line) in the 4 μm wide track. Data corresponding to the empty stars are taken from Ref. 9.

Case 2 (Steady State corr.): Tracks are assumed to have reached the stationary state at the end of the pulses: $T_i(J) = 95\,\mathrm{K} - \Delta T(J, \infty)$. This correction of Joule heating leads to an overestimation of the temperature rise, increasing with J, since the final temperature is not constant ($T_f(J) = 95\,\mathrm{K} + \Delta T(J, 1\mu s) - \Delta T(J, \infty) < 95\,\mathrm{K}$).

Case 3 (Uncorrected): The track temperature rises are not taken into account. $T_i(J) = 95\,\mathrm{K}$ is kept constant whatever J. In this case, the track become increasingly warmer with J, as $T_f(J) = 95\,\mathrm{K} + \Delta T(J, 1\,\mu s) > 95\,\mathrm{K}$.

Domain wall velocities v measured as a function of J are reported in Fig. 6, for the three corrections and for a constant pulse duration ($\Delta t = 1\,\mu s$). Let us focus on the results obtained with the 4 μm wide track (filled symbols). For $J < 5\,\mathrm{GA/m^2}$, the curves are superimposed. In particular, the threshold value ($J \approx 2\,\mathrm{GA/m^2}$) for DW-motion is observed to be independent of Joule heating. Above $\approx 2\,\mathrm{GA/m^2}$, the curves split: the DW velocity becomes higher (lower) for case 3 (case 2) compared to case 1. Therefore, the Joule heating modifies notably the observed DW dynamics. The slope increase as the final track temperature increases (from case 2 to 3) most probably reflects the temperature dependence of the current DW mobility ($\mu_J = v/J$).[8,9] Similar results (not shown) are observed for the 2 μm wide track.

For the interpretation of DW dynamics, it is crucial to discriminate pinning dependent regimes (creep and depinning regimes) from dissipative regimes (flow regimes). In order to address this point, we can compare the DW dynamics and in tracks presenting different pinning characteristics undergoing different temperature rises for identical current density. Between 2 and 4 μm wide tracks, the dissipated power and the temperature rise ΔT are expected to vary by a factor ≈ 2. A comparison of the DW dynamics is reported in Fig. 6. At low J, DWs are pinned and their velocity $v \approx 0\,\mathrm{m/s}$. The DW-velocity starts to increase significantly for $J \approx 2$ and 5 $\mathrm{GA/m^2}$, for the 4 and 2 μm tracks, respectively. As those threshold values are almost independent of ΔT, this indicates that the pinning of DWs is stronger in the 2 μm wide track. Above those thresholds, it is not straightforward to determine for each track the current density corresponding to the end of pinning dependent regimes. However, for $J > 11\,\mathrm{GA/m^2}$, both curves are superimposed. In this regime, the DW velocity is independent of the specific pinning properties of each track. Therefore, the DW dynamics corresponds to a flow regime. Alternatively, this result indicates that the method proposed to correct for the Joule heating (case 1, constant T_f) gives reproducible data whatever the temperature rises. For the 4 μm wide track, the linear common variation extends below $J = 11\,\mathrm{GA/m^2}$, which is compatible with a weaker pinning strength in this track. Within experimental error bars, the curve corresponding to the case 1 can be linearly extrapolated to $v = 0\,\mathrm{m/s}$ for $J \to 0$. This is compatible with the 1D-model predictions.[8,9] On the contrary, the curves corresponding to case 3 does not extrapolate to $v = 0\,\mathrm{m/s}$ but to a finite current density value ($J \approx 2\,\mathrm{GA/m^2}$). This suggests a DW motion in the depinning regime, both controlled by the damping and (extrinsic) DW pinning. Therefore, an inaccurate correction of Joule heating can lead to a misinterpretation of domain wall dynamics.

VI. CONCLUSION

We have shown that the Joule heating is essentially controlled by the diffusion of heat through the interlayer and the substrate located below the track. This work has implications for current-induced DW-motion experiments performed with different track and substrate materials. GaAs and other typical substrates (Al_2O_3, Si, for example) have similar range of heat conductivities ($K \approx 10 - 100\,\mathrm{W/m\,K}$). Therefore, we can discuss orders of magnitude of the time constant and temperature rises more generally involved in current-induced DW-motion experiments.

For pulse durations Δt lower than 1 ms, DW-motion always occur in the transient heating regime. In the 1-10 μs range, the heat diffusion length is of the order $l_D = \sqrt{D\Delta t}$ = 3–30 μm. As this length is much lower than typical substrate thicknesses ($L \approx$ 100–400 μm), the temperature rise varies logarithmically with time, as predicted by Eq. (2). For much shorter pulse durations ($\Delta t \approx 1$ ns), this equation is not valid anymore, as $\Delta t \ll w^2/(D) = 0.1$–100 ns, for typical track widths (w = 100–1000 nm) and diffusion coefficients ($D \approx$ 10–100 $\times 10^{-6}\mathrm{m^2/s}$). Nevertheless, the diffusion length ($l_D = \sqrt{D\Delta t} =$ 100–300 nm) is larger than typical track thicknesses ($h \approx$ 1–10 nm). Therefore, some heat diffuses through the substrate, whose thermal properties control the track temperature rise.

Moreover, for the typical current densities required to move domain walls, the dissipated power is three orders of magnitude larger in metallic systems ($J \approx 10^{12}\mathrm{A/m^2}$, $\rho \approx 1\,\mu\Omega\,\mathrm{cm}$) than in ferromagnetic semiconductors

($J \approx 10^9 \mathrm{A/m^2}$, $\rho \approx 1\,\mathrm{m\Omega\,cm}$). Hence, Joule heating should have an impact on current-induced domain wall dynamics also in metallic tracks. This also raises the issue of heat dissipation in high frequency devices relying on current induced domain wall motion.

ACKNOWLEDGMENTS

This work was partly supported by the French projects RTRA Triangle de la physique Grant Nos. 2009-024T-SeMicMac and 2010-033T-SeMicMagII and performed in the framework of the MANGAS Project (2010-BLANC-0424).

[1]J. C. Slonczewski, J. Magn. Magn. Mater. **12**, 108 (1979).
[2]D. A. Allwood *et al*., Science **309**, 1688 (2005).
[3]S. S. P. Parkin, M. Hayashi, and L. Thomas, Science **320**, 190 (2008).
[4]G. Tatara, H. Kohno, and J. Shibata, Phys. Rep. **468**, 213 (2008), and references therein.
[5]M. Yamanouchi, D. Chiba, F. Matsukura, T. Dietl, and H. Ohno, Phys. Rev. Lett. **96**, 096601 (2006).
[6]J.-P. Adam, N. Vernier, J. Ferré, A. Thiaville, V. Jeudy, A. Lemaître, L. Thévenard, and G. Faini, Phys. Rev. B **80**, 193204 (2009).
[7]K. Y. Wang, K. W. Edmonds, A. C. Irvine, G. Tatara, E. De Ranieri, J. Wunderlich, K. Olejnik, A. W. Rushforth, R. P. Campion, and D. A. Williams, Appl. Phys. Lett. **97**, 262102 (2010).
[8]V. Jeudy, J. Curiale, J.-P. Adam, A. Thiaville, A. Lemaître, and G. Faini, J. Phys.: Condens. Matter **23**, 446004 (2011).
[9]J. Curiale, A. Lemaître, C. Ulysse, G. Faini, and V. Jeudy, Phys. Rev. Lett. **108**, 076604 (2012).
[10]I. M. Miron *et al*., Nature Mater. **10**, 419 (2011).
[11]N. Vernier, D. A. Allwood, D. Atkinson, M. D. Cooke, and R. P. Cowburn, Europhys. Lett. **65**, 526 (2004).
[12]A. Yamaguchi, S. Nasu, H. Tanigawa, T. Ono, K. Miyake, K. Mibu, and T. Shinjo, Appl. Phys. Lett. **86**, 012511 (2005).
[13]A. Yamaguchi, A. Hirohata, T. Ono, and H. Miyajima, J. Phys.: Condens. Matter **24**, 024201 (2012).
[14]S. Emori and G. S. D. Beach, J. Phys.: Condens. Matter **24**, 024214 (2012).
[15]C.-Y. You, I. M. Sung, and B.-K. Joe, Appl. Phys. Lett. **89**, 222513 (2006).
[16]K.-J. Kim, J.-C. Lee, S.-B. Choe, and K.-H. Shin, Appl. Phys. Lett. **92**, 192509 (2008).
[17]C.-Y. You and S.-S. Ha, Appl. Phys. Lett. **91**, 022507 (2007).
[18]J. Curiale, A. Lemaître, G. Faini, and V. Jeudy, Appl. Phys. Lett. **97**, 243505 (2010).
[19]L. Thevenard, L. Largeau, O. Mauguin, G. Patriarche, A. Lemaître, N. Vernier, and J. Ferré, Phys. Rev. B **73**, 195331 (2006).
[20]A. Lemaître, A. Miard, L. Travers, O. Maugin, L. Largeau, C. Gourdon, V. Jeudy, M. Tran, and J.-M. Georges, Appl. Phys. Lett. **93**, 021123 (2008).
[21]J. S. Blakemore, J. Appl. Phys. **53**(10), R123 (1982).
[22]S. Adachi, J. Appl. Phys. **54**, 1844 (1983).
[23]N. N. Sirota, V. V. Novikov, and A. M. Antiukhov, Dokl. Akad. Nauk SSSR **263**, 96 (1982).
[24]See http://www.comsol.com for COMSOL MULTIPHYSICS.
[25]J. Torrejon, G. Malinowski, M. Pelloux, R. Weil, A. Thiaville, J. Curiale, D. Lacour, F. Montaigne, and M. Hehn, Phys. Rev. Lett. **109**, 106601 (2012).
[26]P. M. Haney and M. D. Stiles, Phys. Rev. B **80**, 094418 (2009).
[27]J.-Y. Chauleau, R. Weil, A.Thiaville, and J. Miltat, Phys. Rev. B **82**, 214414(7) (2010).
[28]V. Uhlir *et al*., Phys. Rev. B **81**, 224418 (2010).